Nanoscale functional interlayers formed through spontaneous vertical phase separation in polymer photovoltaic devices

Fang-Chung Chen*[a] and Shang-Chieh Chien[b]

Received 17th April 2009, Accepted 3rd July 2009
First published as an Advance Article on the web 30th July 2009
DOI: 10.1039/b907773a

A nanoscale interlayer formed through spontaneous vertical phase separation enhances the efficiency and stability of polymer solar cells. Poly(ethylene glycol) molecules blended into the photoactive layer spontaneously migrate to the surface of the polymer blend to form the interfacial buffer, thereby reducing the contact resistance after undergoing chemical reactions with the Al atoms of the cathode. The vertical phase separation of PEG molecules in the device were investigated by using depth profiling scanning electron microscopy and atomic force microscopy.

With the rise in awareness of global environmental issues, the development of sources of renewable energy, such as solar energy, is attracting increasing attention. Among the various kinds of renewable energy sources using the solar cell technologies, organic photovoltaic devices (OPVs) based on conjugated polymer materials[1,2] are promising systems because they feature many advantageous properties, including light weight, mechanical flexibility, and low-temperature and low-cost fabrication of large-area devices. The most efficient OPVs fabricated to date are based on bulk heterojunction structures prepared through the blending of conjugated polymers and fullerenes, which form an interpenetrating network having a high density of interfaces. The morphology of the bulk heterojunction significantly affects the efficiencies of exciton dissociation and charge transportation and, in turn, the power conversion efficiency (PCE). To achieve high efficiency, the morphology of the blends—for example, those prepared from poly(3-hexylthiophene) (P3HT) and [6,6]-phenyl-C_{61}-butyric acid methyl ester (PCBM)—can be improved through such approaches as solvent annealing,[3] thermal annealing,[4] and microwave annealing.[5] Another key issue is the creation of effective metal–organic interfaces that decrease the contact resistance and enhance the charge collection efficiency. Possible approaches include the insertion of low-work-function metals or insulating interlayers (*e.g.*, LiF,[6] Cs_2CO_3,[7,8] or TiO_x[9]) between the organic materials and the cathodes. Nevertheless, the instability of these materials under ambient atmosphere usually leads to degraded device performance. Therefore, a need remains to develop an interfacial material that can provide OPVs with both high efficiency and superior stability.

Recently, vertical segregation between organic molecules and its application toward improving the performance of organic electronic devices have became subjects of intense research activity.[10–13] For example, Goffri *et al.* reported high-performance organic thin film transistors (OTFTs) containing spontaneously formed bilayer structures from a binary mixture of P3HT and polyethylene.[10] To improve the stability of OTFTs, Arias *et al.* also demonstrated the self-encapsulation of air-stable OTFTs by depositing a blend of polymeric semiconductor and poly(methyl methacrylate) (PMMA), with the latter preferentially segregating from the blend to the top of the surface PMMA and serving as the encapsulant.[11] Similarly, Qiu *et al.* developed a P3HT-top and PMMA-bottom structure by controlling the surface energy of the substrate.[12] More recently, Wei *et al.* reported high-performance OPVs containing a fullerene derivative presenting fluorocarbon side chains (F-PCBM), which became a buffer layer between the photoactive layer and the cathode metal through spontaneous surface segregation.[13] Nevertheless, relevant reports concerning the application of self-organization phenomena to the production of OPVs are rare.

Previously, Zhang *et al.* reported the application of nonconjugated polymers (surfactant), such as poly(ethylene oxide) (PEO), as buffer layers between the active polymer layer and the metal cathode to improve the device performance of polymer solar cells.[14] They attributed the enhancement to the impact on the internal electrical field, thereby improving charge transportation. Although spin-coating is a convenient method for preparing the PEO layer, it adds an additional step to the fabrication process. In this study, we introduced a nanoscale functional interlayer, containing poly(ethylene glycol) (PEG), through spontaneous vertical phase separation to enhance the efficiency and increase the stability of polymer solar cells (Fig. 1). During spin-coating, the PEG molecules migrated to the surface and formed a thin layer on top of the active polymer film. The preferential segregation of PEG molecules on the P3HT:PCBM layer allowed the direct formation of a nanoscale functional buffer layer between the P3HT:PCBM thin film and the high-work-function metal (Al) in the polymer solar cells without the need for an additional fabrication step (*e.g.*, spin-coating or thermal evaporation). After thermal deposition, the chemical interaction between the PEG monolayer and the Al atoms lowered the interfacial barrier height and contact resistance and, thereby, enhanced the device performance. This approach allows the ready preparation of bilayer structures in a single fabrication step. Moreover, the resulting polymer photovoltaic devices exhibit both higher PCE and superior device operating stability.

The process flow of the polymer solar cells is illustrated in Fig. 1. The device consists of a typical sandwich structure.

[a]*Department of Photonics & Display Institute, National Chiao Tung University, Hsinchu, 30010, Taiwan. E-mail: fcchen@mail.nctu.edu.tw*
[b]*Department of Photonics & Institute of Electro-optical Engineering, National Chiao Tung University, Hsinchu, 30010, Taiwan*

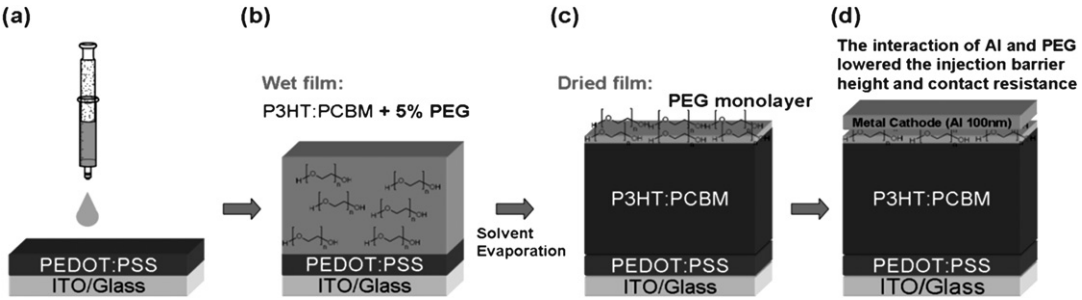

Fig. 1 Schematic representation of the fabrication processes of solar cells featuring a self-organized bilayer (P3HT:PCBM/PEG) structure.

The solar cells were made on indium tin oxide (ITO)-coated glass substrates. The ITO substrates underwent a routine cleaning procedure, which included sonication in a detergent followed by repeated rinsing sequentially in deionized water, acetone, and isopropanol. After cleaning, the substrates were treated with UV-Ozone. Poly(3,4-ethylenedioxythiophene):poly(styrene sulfonate) (PEDOT:PSS; Baytron® PVP P) was spin-coated onto the ITO substrates. After annealing the PEDOT:PSS layer at 120 °C for 1 h, P3HT/PCBM (1:1, w/w) blends dissolved in 1,2-dichlorobenzene were spin-coated on the PEDOT:PSS layer to form 110 (±10)-nm-thick active layers. Finally, the cathode—Al (100 nm), Ca (50 nm)/Al (100 nm), or LiF (0.8 nm)/Al (100 nm)—was formed through thermal evaporation at a pressure of *ca.* 5×10^{-6} torr. For the preparation of devices containing PEG (Fluka; $M_n = 1500$), the polymer was blended into the active layer at a weight ratio of 5, 10, or 20%. The *J*–*V* curves were measured using the Keithley 2400 measurement system; the photocurrents were obtained under illumination with a Thermal Oriel solar simulator (AM1.5G). The illumination intensity was calibrated using a standard Si photodiode detector equipped with a KG-5 filter (Hamamatsu, Inc). The calibration method, based on the IEC-69094-1 spectrum, followed procedures described previously.[15] More than ten batches of devices were made for each device category. According to our experimental results, the devices were quite reproducible and repeatable. Therefore, the results were then analyzed and averaged; the data shown in this paper shows the representative results. SEM images were recorded using a JEOL (Tokyo, Japan) JSM-7041 field emission scanning electron microscope equipped with an Oxford INCA energy 350 system and operated at electron accelerating voltages of 10kV. Sample etching was performed using Ar^+ ions at an accelerating voltage of 3 kV; the etching rate was *ca.* 0.1 nm/s. The thickness of the removed film of the active layer was calculated from the etching time. The film phase morphology was analyzed using a DI 3100 series.

Fig. 2 presents the current density–voltage (*J*–*V*) curves for devices based on Al cathodes prepared with and without PEG incorporated in the active layer under illumination with simulated solar irradiation (AM 1.5G) at 100 mW/cm^2. The standard device, which was fabricated without PEG, exhibited a short circuit current density (J_{sc}) of 8.36 mA/cm^2, an open circuit voltage (V_{oc}) of 0.49 V, and a fill factor (FF) of 53.9%, corresponding to a PCE of 2.21%. After the addition of PEG (5 wt%) into the active layer, the device performance improved considerably: the corresponding values of J_{sc}, V_{oc}, and FF were 12.12 mA/cm^2, 0.59V, and 55.5%, respectively, and the calculated PCE was 3.97%. We speculate that the enhanced device performance originated from interactions between PEG and Al that reduced the injection barrier height and contact resistance between the polymer layer and the cathode metal and, thereby, improved the efficiency of electron collection.

The improved values of J_{sc} and FF imply a significant reduction in the device's series resistance (R_s), which includes the bulk resistance of the organic layers and the contact resistances between the polymer layers and electrodes. We derived the value of R_s of each device from the slopes of the *J*–*V* curves recorded in the dark;[16] it decreased from 12.51 to 5.88 Ω cm^2 after blending PEG into the device. Many reports describe how the efficiency of charge injection can be improved through the use of PEG because of its strong interactions with Al metal.[17–19] Therefore, we suspect that this reduction in device resistance was due mainly to decreased contact resistance between the active layer and the Al electrode after the chemical interaction between PEG and Al.[17–21] In contrast, a tremendous drop in device performance—to below that of the standard device—occurred when we increased the concentration of PEG to 10 wt% (Fig. 2). Because PEG is insulating, it is not surprising that too many PEG molecules would increase the device series resistance (R_s = 65.7 Ω cm^2), thereby lowering the FF to 45%. A further increase in concentration to 20% provided an extremely poor device performance, with the value of R_s increasing to 10,500 Ω cm^2 (Fig. 2).

To investigate the distribution of PEG molecules in the polymer blend, we recorded scanning electron microscopy (SEM) images of the P3HT:PCBM films prepared with and without

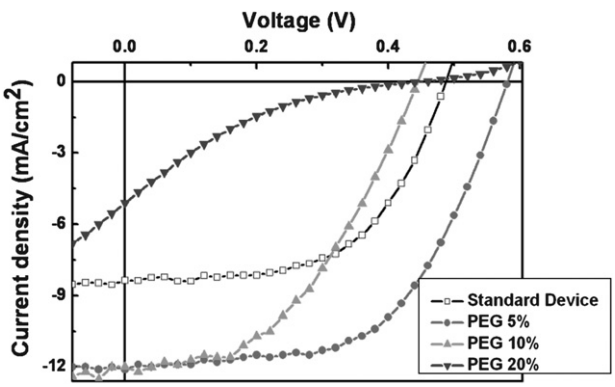

Fig. 2 Current density–voltage (*J*–*V*) plots of devices prepared with and without PEG, measured under illumination (simulated AM1.5G) at 100 mW/cm^2.

PEG (Fig. 3a–c). The film containing no PEG [Fig. 3(a)] exhibits a smooth surface morphology. After blending 5% PEG into the film, a "dot-like" phase was present on surface of the film, with features having an average diameter of *ca.* 30 nm [Fig. 3(b)]. When the PEG concentration was 10%, the new phase, which we suspect was composed of PEG polymer, covered almost the entire surface [Fig. 3(c)]. Because the densities of the three components in the polymer composites are similar, we would not expect the PEG phase to cover the whole surface at a concentration of only 10%. Therefore, we suspect that the distribution of PEG molecules was uneven and that phase separation in a direction normal to the substrate occurred in the thin films.

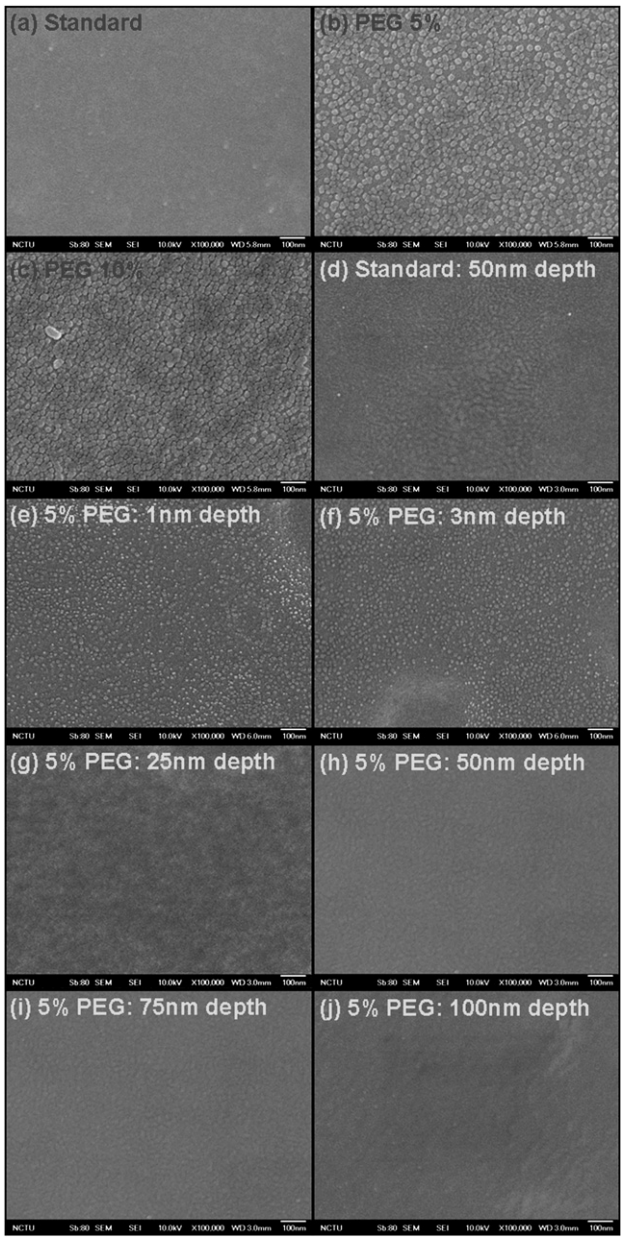

Fig. 3 (a–c) SEM images of the surfaces of the active layers prepared at PEG concentrations of (a) 0, (b) 5, and (c) 10%. (d–j) SEM depth-profile images of the active layers at depths of (d) 50 nm (for the thin film prepared without PEG) and (e) 1, (f) 3, (g) 25, (h) 50, (i) 75, and (j) 100 nm (for the thin film containing 5% PEG).

The vertical phase separation observed in the SEM images is consistent with the device performance in Fig. 2. When the concentration of PEG was 5%, the thin interlayer would react with evaporated Al atoms, thereby reducing the device contact resistance. As a result, we obtained a higher photocurrent and PCE. An even higher concentration (10%) would, however, result in a thick insulator layer,[22,23] leading to an increased contact series resistance and, therefore, a decreased photocurrent (Fig. 2). At a PEG concentration of 20%, the surface of the thin films was covered entirely by the insulator, resulting in a very poor device performance.

In order to further investigate the vertical-type phase separation, we recorded depth-profile SEM images of the bulk heterojunction films to measure the distribution of PEG molecules. To obtain SEM images at various depths, we etched the samples, using Ar^+ ions at an accelerating voltage of 3 kV, at a rate of *ca.* 0.1 nm/s. Fig. 3(e)–(j) display the SEM images of the film incorporating 5% PEG after various etching times; the image of the film prepared without PEG is provided in Fig. 3(d) as a reference. After etching for 10 and 30 s (corresponding to layer thicknesses of *ca.* 1 and 3 nm, respectively), we still observed the dot-like features, but with fewer dots of smaller size (*ca.* 10 nm) [Fig. 3(e) and (f), respectively]. In Fig. 3(f), some regions exist that contain no PEG phase. Deeper into the film (>25 nm), the PEG phase completely disappeared [Fig. 3(g)–(j)]; the images are similar to that recorded at the depth of 50 nm for the film prepared in the absence of PEG [Fig. 3(d)]. These results imply that the PEG molecules tended to migrate to the top of the surface and existed only at the surface (*ca.* 3 nm) of the composite films.

Fig. 4(a) and (b) display phase images of the polymer films prepared in the absence and presence (5%) of PEG, respectively; we observe significantly different morphologies, suggesting that different materials existed on the surface. Because PEG readily dissolves in water, whereas P3HT and PCBM exhibit limited solubility, we dipped the composite film of P3HT, PCBM, and 5% PEG into water to wash away the PEG molecules. Fig. 4(c) displays the phase morphology of the polymer film obtained after such treatment. The surface, which originally had a quite rough morphology [Fig. 4(b)], became smoother after dissolving the PEG units into water. The surface morphology was almost identical to that of the film prepared without PEG [Fig. 4(a)]—certainly in terms of the surface roughness. Taken together with our SEM images, these images confirmed that a bilayer structure had indeed developed through a vertical separation process, in which PEG units segregated spontaneously to the surface of the polymer blend film.

Because the work function of Al is higher relative to those of other metals (*e.g.*, Ca) that are commonly used as cathode materials for polymer solar cells, we expected the device fabricated solely with Al as the cathode to exhibit lower sensitivity to moisture and oxygen from the ambient atmosphere. Fig. 5 reveals that the time-dependent photocurrent of the Al-cathode device under illumination was comparable to those of conventional devices prepared using Ca/Al and LiF/Al as cathode structures. Note that solar devices featuring a LiF/Al cathode are regarded as possessing very long device lifetimes.[24] Surprisingly,

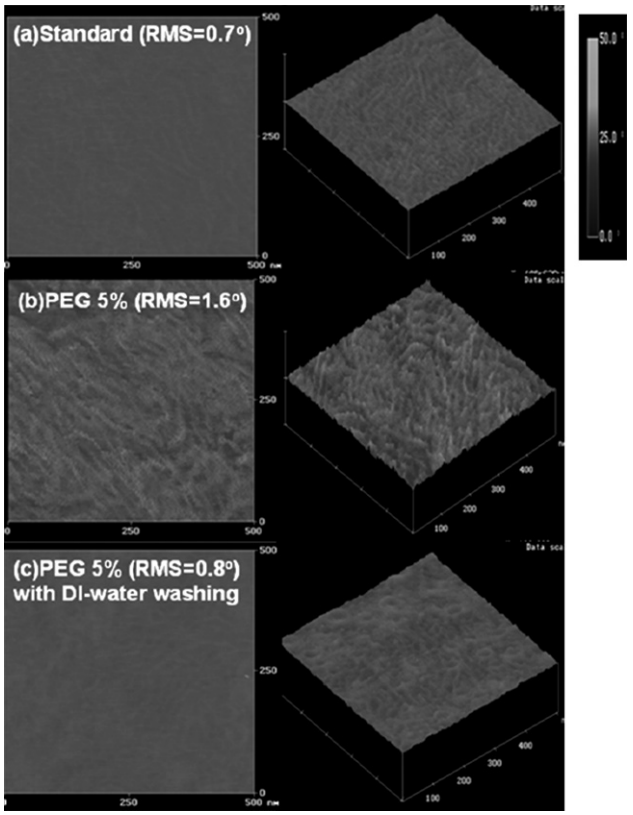

Fig. 4 AFM phase images (0.5 μm × 0.5 μm) of P3HT:PCBM films incorporating (a) 0 and (b, c) 5% PEG; the image in (c) was obtained after the washing of the sample in (b) with DI water.

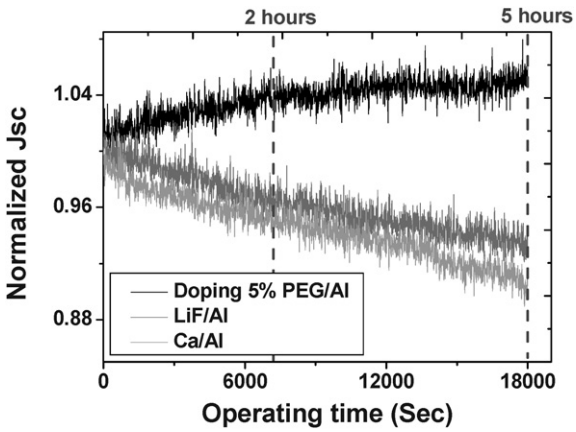

Fig. 5 Photocurrent stability measurements of devices incorporating various cathode structures, under illumination (AM1.5G, 100 mW/cm^2) for 5 h. The initial values of J_{sc} were normalized for ready comparison. The active layers of the devices incorporating LiF/Al and Ca/Al as cathode materials did not contain any PEG.

the value of J_{sc} of the device prepared with 5% PEG increased slightly over time; in contrast, those of the devices based on LiF/Al and Ca/Al cathodes decreased rapidly. Table 1 summarizes the behavior of the three devices measured before and after 5 h of stress. The performances of the devices incorporating the Ca/Al and LiF/Al electrodes did indeed degrade; in contrast, because of its increased photocurrent and FF, the PCE of the

Table 1 Device performances before and after 5 h of stress under illumination at 100 mW/cm^2 (AM 1.5G)

Cathode Structure	Measurement condition[a]	Voc [V]	Jsc [mA/cm^2]	FF [%]	PCE [%]
Self-organized PEG/Al	Before	0.59	12.12	55.5	3.97
	After	0.59	12.67	57.0	4.24
LiF/Al	Before	0.53	9.87	55.8	2.92
	After	0.49	9.27	49.9	2.27
Ca/Al	Before	0.59	8.82	69.2	3.60
	After	0.57	7.71	67.8	2.98

[a] 5 hours of stress under illumination at 100 mW/cm^2 (AM 1.5G).

device containing PEG and the single-layer Al electrode increased unexpectedly to 4.24%. Moreover, the value of V_{oc}, which is related directly to the nature of the contacts,[25] of the device incorporating 5% PEG remained constant (0.59 V), suggesting a high stability for the metal contacts after stress. On the other hand, the values of V_{oc} of the devices incorporating Ca/Al and LiF/Al decreased, indicating the degradation of their cathodes.

In addition to its resistance to oxidation by atmospheric O_2, the superior stability of the PEG-containing device might also be attributable to the stable interface at the cathode, where physical diffusion of the cathode materials is minimized. For Ca/Al and LiF/Al devices, the interlayer materials (*i.e.*, Ca and/or LiF atoms) might diffuse into the polymer layer, thereby degrading the interface. On the other hand, because the PEG molecules preferred to segregate to the top of the polymer film, the contact should be quite thermodynamically stable, thereby inhibiting diffusion through the cathode interface. Therefore, the cathode contact should stay distinctive and effective, leading to a stable open-circuit voltage. We attribute the increase in the value of J_{sc} after 5 h of stress to an orientational effect,[26,27] through which the crystallinity and/or molecular conformation of the P3HT component changed gradually to a preferential direction under the strong electrical field, thereby facilitating the conduction of holes. The bulk resistance decreased accordingly, resulting in improved values of J_{sc} and FF. An in-depth investigation of this effect and an analysis of the morphological evolution are currently in progress.

In addition to the stress test under illumination, for the "storage stability", the device somehow degraded slightly after the devices were stored in the atmosphere for 15 days because the devices were tested in the atmosphere and we only had very simple encapsulation (using UV-cured epoxy). However, the V_{oc} still stayed at 0.59 V. No variation was observed at least for 15 days, suggesting a very stable organic/metal interfaces in the devices.

In conclusion, we have developed a conceptually unique approach toward preparing self-organized bilayer structures in polymer solar cells. It is noteworthy that only a single step is required to fabricate both the active and cathode buffer layers. PEG molecules migrate spontaneously to the surface of the polymer blend to form the interfacial buffer, reducing the contact resistance after undergoing chemical reactions with Al atoms. The performance of the resulting device was enhanced, as measured in terms of the increased values of V_{oc}, J_{sc}, and PCE and the improved stability. Furthermore, unlike conventional

buffer layers, such as LiF, that are prepared through vacuum deposition, this approach allows printing technology to be used for cell fabrication.

Acknowledgements

This study was supported by the National Science Council, Taiwan (NSC 98-2221-E-009-028), and the ATU plan of the Ministry of Education, Taiwan.

References

1 L. M. Chen, Z. Hong, G. Li and Y. Yang, *Adv. Mater.*, 2009, **21**, 1434.
2 J. Peet, M. L. Senatore, A. J. Heeger and G. C. Bazan, *Adv. Mater*, 2009, **21**, 1521.
3 G. Li, V. Shrotriya, J. S. Huang, Y. Yao, T. Moriarty, K. Emery and Y. Yang, *Nat. Mater.*, 2005, **4**, 864.
4 G. Li, V. Shrotriya, Y. Yao and Y. Yang, *J. Appl. Phys.*, 2005, **98**, 043704.
5 C. J. Ko, Y. K. Lin and F. C. Chen, *Adv. Mater.*, 2007, **19**, 3520.
6 E. Ahlswede, J. Hanisch and M. Powalla, *Appl. Phys. Lett.*, 2007, **90**, 163504.
7 H. H. Liao, L. M. Chen, Z. Xu, G. Li and Y. Yang, *Appl. Phys. Lett.*, 2008, **92**, 173303.
8 F. C. Chen, J. L. Wu, S. S. Yang, K. H. Hsieh and W. C. Chen, *J. Appl. Phys.*, 2008, **103**, 103721.
9 J. Y. Kim, S. H. Kim, H. H. Lee, K. Lee, W. L. Ma, X. Gong and A. J. Heeger, *Adv. Mater.*, 2006, **18**, 572.
10 S. Goffri, C. Muller, N. Stingelin-Stutzmann, D. W. Breiby, C. P. Radano, J. W. Andreasen, R. Thompson, R. A. J. Janssen, M. M. Nielsen, P. Smith and H. Sirringhaus, *Nat. Mater.*, 2006, **5**, 950.
11 A. C. Arias, F. Endicott and R. A. Street, *Adv. Mater.*, 2006, **18**, 2900.
12 L. Qiu, J. A. Lim, X. Wang, W. H. Lee, M. Hwang and K. Cho, *Adv. Mater.*, 2008, **20**, 1141.
13 Q. S. Wei, T. Nishizawa, K. Tajima and K. Hashimoto, *Adv. Mater.*, 2008, **20**, 2250.
14 T. Zhang, M. Ceder and O. Inganas, *Adv. Mater.*, 2007, **19**, 1835.
15 V. Shrotriya, G. Li, Y. Yao, T. Moriarty, K. Emery and Y. Yang, *Adv. Funct. Mater.*, 2006, **16**, 2016.
16 D. W. Sievers, V. Shrotriya and Y. Yang, *J. Appl. Phys.*, 2006, **100**, 114509.
17 X. Y. Deng, W. M. Lau, K. Y. Wong, K. H. Low, H. F. Chow and Y. Cao, *Appl. Phys. Lett.*, 2004, **84**, 3522.
18 Y. H. Niu, H. Ma, Q. M. Xu and A. K. Y. Jen, *Appl. Phys. Lett.*, 2005, **86**, 083504.
19 T. F. Guo, F. S. Yang, Z. J. Tsai, T. C. Wen, S. N. Hsieh, Y. S. Fu and C. T. Chung, *Appl. Phys. Lett.*, 2006, **88**, 113501.
20 F. C. Chen, S. C. Chien and S. W. Lee, *Electrochem. Solid-State Lett.*, 2008, **11**, J50.
21 F. C. Chen, S. C. Chien and Y. S. Chen, *Appl. Phys. Lett.*, 2009, **94**, 043306.
22 S. E. Shaheen, G. E. Jabbour, M. M. Morrell, Y. Kawabe, B. Kippelen, N. Peyghambarian, M. F. Nabor, R. Schlaf, E. A. Mash and N. R. Armstrong, *J. Appl. Phys.*, 1998, **84**, 2324.
23 Y. D. Jin, X. B. Ding, J. Reynaert, V. I. Arkhipov, G. Borghs, P. L. Heremans and M. Van der Auweraer, *Org. Electron.*, 2004, **5**, 271.
24 R. De Bettignies, J. Leroy, M. Firon and C. Sentein, *Synth. Met.*, 2006, **156**, 510.
25 C. J. Brabec, A. Cravino, D. Meissner, N. S. Sariciftci, T. Fromherz, M. T. Rispens, L. Sanchez and J. C. Hummelen, *Adv. Funct. Mater.*, 2001, **11**, 374.
26 F. Padinger, R. S. Rittberger and N. S. Sariciftci, *Adv. Funct. Mater.*, 2003, **13**, 85.
27 T. F. Guo and Y. Yang, *Appl. Phys. Lett.*, 2002, **80**, 148.